

[Chem. Pharm. Bull.]
34(7)2698—2709(1986)

Thermodynamic and Viscometric Studies on the Thermotropic Phase-Stability of Cholesteryl Myristate, Palmitate, Stearate, and Oleate

HIROSHI KISHIMOTO,* TAKAO IWASAKI, and MASAKATSU YONESE

Faculty of Pharmaceutical Sciences, Nagoya City University,
Tanabe-dori, Mizuho-ku, Nagoya 467, Japan

(Received December 24, 1985)

By means of differential scanning calorimetry and polarizing microscopy, the transition paths, temperatures, enthalpies and isopiestic heat capacities were measured for four mesogenic esters, *i.e.* cholesteryl myristate (ChM), palmitate (ChP), stearate (ChS), and oleate (ChO). By using the above-mentioned thermodynamic quantities, relative chemical potential diagrams were constructed to clarify the thermodynamic phase stability of each ester. The viscosity behavior of each ester was measured at various temperatures under various conditions: continuous heating and cooling as well as isothermal. The effect of thermal history before the isothermal measurements was also examined. On the basis of chemical potential and viscometric diagrams, the phase stability of each ester with or without the influence of shear in the viscometer is discussed. Each ester in cholesteric phase was estimated to behave as a "continuum" without shear, but as a "swarm" under shear. The nature of the peak or hump in the transition region between isotropic and cholesteric phases is also discussed.

Keywords—cholesteryl myristate; cholesteryl palmitate; cholesteryl stearate; cholesteryl oleate; DSC; viscometry; chemical potential; phase stability; hysteresis; liquid crystal

Introduction

Cholesteryl esters with various fatty acids have two *meso*-phases (or liquid crystals), *i.e.* smectic and cholesteric phases (hereafter referred to as *s* and *c*, respectively), as well as normal crystalline and isotropic liquid phases (*k* and *i*).¹⁾ Such a polymorphism of cholesteryl esters and the consequent characteristic properties are of interest in the medicinal and biological fields, because of the significance of liquid crystals in living systems, such as in biomembranes.^{2b)} For this reason, we have studied the thermodynamic as well as rheological properties of cholesteryl myristate, palmitate, stearate, and oleate (ChM, ChP, ChS, and ChO, respectively) under various conditions.³⁻⁵⁾ In the rheological studies of ChM, ChP, and ChO, a problem remained to be settled: the cause of the viscosity maxima found in the transition from *c* to *i*.⁴⁾ Previously, Porter and his co-workers⁶⁾ adopted Lawrence's hypothesis⁷⁾ of a turbulent effect as the cause. However, there are other opinions, such as the molecular considerations of Tamamushi and Matsumoto,⁸⁾ although they concentrated on ammonium laurate, a thermotropic liquid crystalline substance, in the transition from *s* to *i*. Another problem is that similar transition paths of these esters were assumed, regardless of the shear induced in the viscometry procedures used by all the authors mentioned above. Recently, we examined the transition paths of ChO in terms of a thermodynamic parameter, relative chemical potential, μ_{rel} , and proposed an explanation for the phase-stability of ChO in various states.⁵⁾ In this work, in an attempt to solve the above-mentioned problems, we deal with the viscometric phase-stability of ChM, ChP, ChS, and ChO based upon diagrams of μ_{rel} vs. temperature, which were constructed by using differential scanning calorimetry (DSC) data. We also examined the kinetic behavior through the measurements of the carbon-13 nuclear magnetic resonance (¹³C-NMR) spectra as well as isothermal viscosity time-courses.

Experimental

Materials—ChM, ChP, ChS, and ChO were obtained from Tokyo Chem. Ind. Co. These esters will be generically referred to as "esters" in this work. ChM, ChP, and ChS were each recrystallized four times from ethanol and ChO was recrystallized twice from ethanol and twice from 1-pentanol.⁵⁾ After being dried *in vacuo* at room temperature for several days, they were stored in nitrogen-filled containers at *ca.* 275 K before use. Ethanol and 1-pentanol from Katayama Chem. Ind. Co. (G.R.) were twice distilled before use.

Apparatus and Procedures—DSC: To study the thermal behavior of esters, we used a differential scanning calorimeter (Seiko Instruments & Electronics Ltd., SSC 560U), following the same procedure as previously.⁵⁾

Polarizing Microscopy (PM): Transition characteristics of esters were observed by using a polarizing microscope (Olympus Optical Co., Model POS) with a hot stage (Mettler Instrumente A. G., Model FP5, FP52) between crossed polarizers.⁵⁾

Viscometry: Viscosity was measured by means of a cone-plate type instrument (Tokyo Keiki Co., E-type viscometer). The cone angle and the radius of the rotator were 3° and 1.4 cm, respectively. The shear rate was maintained at 10 s⁻¹. The sample application, temperature control, and viscosity measurement followed the procedures adopted in the previous work.⁴⁾ Three kinds of measurements were carried out with respect to temperature, *T*, *i.e.* measurements (1) with continuous heating at a mean rate of 0.3 K min⁻¹, (2) with continuous cooling at a mean rate of 0.6 K min⁻¹, and (3) under isothermal conditions. Usually, the measurement of viscosity during continuous cooling was done immediately after that during continuous heating. Before any viscosity measurement to be carried out at constant temperature, a fresh sample was taken and subjected to various kinds of thermal pretreatments, which will be separately described with the respective results, later.

NMR: The ¹³C-NMR spectra of ChO were measured at various temperatures by using an FX-100 pulse Fourier-transform NMR spectrometer.

Results and Discussion

Thermodynamic Parameters of Phase Transitions of Cholesteryl Esters

The thermotropic transition paths of the esters, which were found by means of DSC and PM above room temperature, agreed well with our previous results³⁻⁵⁾ and those of other authors,⁶⁾ and are shown in Chart 1. For ChO, *k*₁ and *k*₂ denote two kinds of polymorphic crystalline phases.⁵⁾ Other than the transitions from *s* to *k* (or *k*₁ and *k*₂) for ChP, ChS, and ChO, all transitions shown in Chart 1 are thermodynamically reversible, although the transition from *k* to *c* (abbreviated as *k/c*) of ChP, *k/i* of ChS, and *k*₁/*i* or *k*₂/*i* of ChO, are monotropic and their reverse paths, *i.e.* *c/k*, *i/k*, and *i/k*₁ or *i/k*₂, respectively, cannot be actually observed.

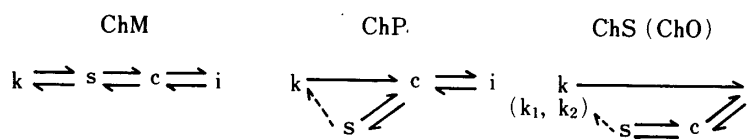


Chart 1. The Phase Transition Diagrams of Cholesteryl Esters

k, crystalline phase; *k*₁ and *k*₂, crystals with higher and lower melting temperatures, respectively; *s*, smectic phase; *c*, cholesteric phase; *i*, isotropic phase.^{1,5)} The diagram for ChO is the same as that for ChS, except that *k*₁ and *k*₂ were found for ChO in place of a single *k* for ChS. Arrows with solid shafts denote thermodynamically reversible phase-transitions. Arrow-heads indicate heating or cooling when directed to the right or left, respectively. The transitions, *k/c* for ChP, *k/i* for ChS, and *k*₁/*i* or *k*₂/*i* for ChO are monotropic changes. The broken arrows denote irreversible transitions accompanied by supercooling.

The transition temperatures, *T*^{*}, molar enthalpies, ΔH_2^* , and isopiestic molar heat capacities, ΔC_p , which were measured by using DSC, are shown in Table I. The above values of *T*^{*} coincided with those observed through PM. Since the heat capacities, *C*_{*p*}, of both phases relevant to each transition varied more or less with temperature, we averaged them in the measured ranges of temperature, before obtaining the difference between them as ΔC_p .⁵⁾

TABLE I. Thermodynamic Parameters of Phase Transitions of Cholesteryl Esters

Ester	Myristate			Palmitate		
	k/s	s/c	c/i	k/c	s/c	c/i
Transition ^{a)}						
$\frac{T^{*b})}{\text{K}}$	344.6	353.0	358.3	350.4	349.9	355.0
$\frac{\Delta H_2^{*c})}{\text{kJ}\cdot\text{mol}^{-1}}$	47.1 ^{d)}	1.6 ^{e)}	1.1 ^{e)}	56.2 ^{d)}	1.7 ^{e)}	1.3 ^{e)}
$\frac{\Delta C_p^{f})}{\text{kJ}\cdot\text{mol}^{-1}\cdot\text{K}^{-1}}$	0.14	0.19	-0.16	0.46	0.18	-0.37

Ester	Stearate			Oleate			
	k/i	s/c	c/i	k ₁ /i	k ₂ /i	s/c	c/i
Transition ^{a)}							
$\frac{T^{*b})}{\text{K}}$	355.4	349.0	353.0	321.2	317.4	315.9	321.0
$\frac{\Delta H_2^{*c})}{\text{kJ}\cdot\text{mol}^{-1}}$	67.5 ^{d)}	1.8 ^{e)}	1.7 ^{e)}	29.0 ^{d)}	27.0 ^{e)}	1.3 ^{e)}	0.84 ^{e)}
$\frac{\Delta C_p^{f})}{\text{kJ}\cdot\text{mol}^{-1}\cdot\text{K}^{-1}}$	0.19	0.11	-0.40	0.21	0.20	0.09	-0.09

a) e.g., k/s denotes the transition from k to s. b) Transition temperature. S.D. 0.1 K. c) Molar enthalpy of transition. d) S.D. 0.3 kJ·mol⁻¹. e) S.D. 0.1 kJ·mol⁻¹. f) Isopiestic molar heat capacity of transition. S.D. 0.02 kJ·mol⁻¹·K⁻¹.

Thermodynamic Phase-Stability of Cholesteryl Esters from the Viewpoint of Relative Chemical Potential

In the preceding work,⁵⁾ we introduced a relative thermodynamic quantity, which can be used to compare thermodynamically the stability of various phases of ChO with some advantage over the usual chemical potential, μ . The quantity or relative chemical potential, μ_{rel} , is defined by Eq. 1.

$$\mu_{\text{rel}} = \mu - \mu_0 + s_0(T - T_0) \quad (1)$$

where μ_{rel} and μ stand for any phase to be compared at the same temperature, T , but μ_0 denotes the chemical potential of ChO at an arbitrarily selected reference state of phase and temperature, e.g. k₁ and 300 K, respectively, and s_0 denotes the molar entropy of ChO at the same state as μ_0 . To calculate the value of μ_{rel} of ChO existing really or imaginarily in any phase at T , the value of C_p in the reference phase as well as the relevant thermodynamic parameters of transition such as T^* , ΔH^* , and ΔC_p were used according to the phase to be considered. The paths, as shown in Chart 1, were also taken into consideration. It should be noted here that the determination of μ_{rel} requires no knowledge of μ , μ_0 , and s_0 , in spite of the formulation of Eq. 1.⁵⁾

In this work, on the same principle as was applied to ChO, we constructed the diagrams of μ_{rel} vs. T for ChM, ChP, and ChS, by using the values of C_p for the reference phase, k (ca. 0.38, 0.71, and 0.61 kJ K⁻¹ mol⁻¹, respectively), as well as the data of Table I. For the sake of clarity, we redrew the relation of μ_{rel} to T among phases to provide a rather schematic representation, magnifying the difference between the slopes of two curves crossing at s/c or

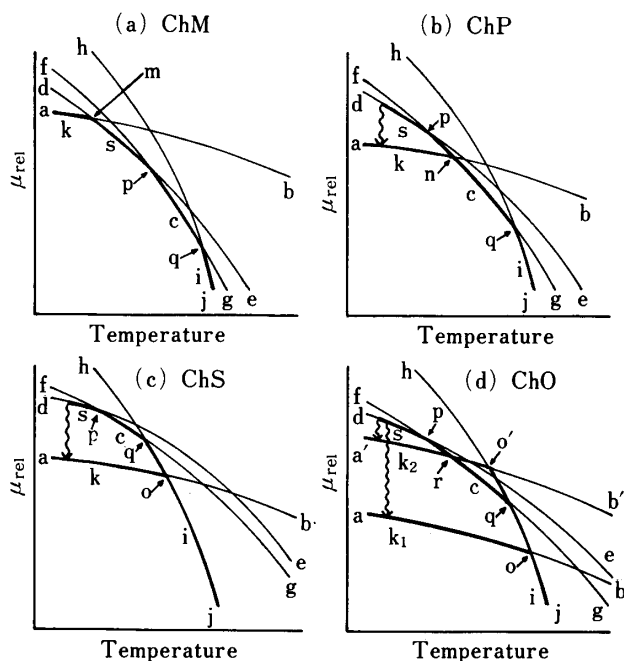


Fig. 1. Schematic Diagrams of Relative Chemical Potential, μ_{rel} , vs. Temperature Relationship

The ordinate shows schematically the qualitative relation of μ_{rel} among phases. See text. Curve a—b, k or k_1 ; a'—b', k_2 ; d—e, s; f—g, c; h—j, i. Crossing m, k/s transition; n, k/c; o, k/i or k_1/i ; o', k_2/i ; p, s/c; q, c/i. Thickened parts of curves indicate the phases observed by means of DSC and PM in the corresponding regions of temperature. The arrows with wave shafts show the possible paths of irreversible phase-transitions. The transition k_2/c for ChO, which was suggested in viscometry, is shown by the crossing r.

c/i transition more than at k/s or k/i transition without altering the relative positions of curves, as shown in Fig. 1(a)—(c). Similarly, we redrew in Fig. 1(d) the diagram of μ_{rel} vs. T for ChO taken from our previous work,⁵ where the figure was drawn to make the difference between the two slopes at each transition proportional to entropy or $\Delta H^*/T^*$. Clearly, among various phases, the curve, whose μ_{rel} is the lowest at any temperature, corresponds to the thermodynamically stable phase at that temperature. The phases corresponding to other curves at that temperature are considered to be thermodynamically unstable and cannot exist, except in temporary meta-stable states.

The phases which were actually observed by DSC and PM are indicated by the thick curves in Fig. 1, which corresponds to the observed region of phase and temperature. As expected, all the thermodynamically stable phases were observed in our experimental range of temperature. However, frequently, especially in cooling paths, some meta-stable phases appeared, as shown by the existence of thickened curves at higher positions in Fig. 1(b), (c), and (d). The appearance of such a meta-stable phase is considered to result from the following processes of a thermotropic system under cooling: by over-passing the transition point between two thermodynamically stable phases, the system remains for a while in the former phase or a meta-stable phase, usually with a transition to another meta-stable phase at lower temperature and sometimes with another transition to a second meta-stable phase.

As an example, we shall discuss the thermotropic behavior of ChS shown in Chart 1 as well as in Fig. 1(c). By heating ChS in phase k, we followed its phase behavior along the thermodynamically stable paths, curve a—o in k and curve o—j in i, with the transition of k/i at the crossing of both curves. In the construction of Fig. 1(c), the transition k/i was considered to be thermodynamically reversible and the molar transition entropy, ΔS^* , was calculated through the division of ΔH^* by T^* . By cooling ChS in phase i, the following processes were found. After over-passing the transition point, o, which would lead to the thermodynamically stable phase, k, and maintaining the same phase, i, along curve j—q, ChS changes its phase to the meta-stable c at q, proceeds along q—p and makes the next transition to another meta-stable phase s. Although the phases, c and s, are meta-stable within the temperature regions of their existence, the transitions, i/c and c/s, are thermodynamically reversible, or the μ_{rel} of the two coexisting phases, i and c for i/c as well as c and s for c/s, are equal to each other at the respective transition temperatures, thereby permitting the

evaluation of ΔS^* of both transitions in the same way as for the k/i transition. In the DSC pan with a cooling rate of *ca.* 0.5 K min^{-1} , ChS changes its phase from s to k a little (*e.g.* 1 K) below the transition temperature for c/s. The transition, s/k, is thermodynamically irreversible and its temperature depends upon the various experimental conditions. Before the irreversible transition, s/k, ChS is heated to change its phase from s to c to i reversibly along the paths from i to c to s. Thus, the transitions, s/c and c/i, are enantiotropic in terms of polymorphism. The kinetic barrier, possibly in the period of nucleus or embryo formation for a new phase, against the transition from c to k is considered to be much higher than the barriers against the s/c and c/i transitions in both directions, on heating and cooling. From the very small values of ΔS^* , which can be estimated by using the data in Table I, and each of which is a measure of the difference of orders between the two phases at transition, and also from the enantiotropicity with the good agreement between the measured T^* on heating and on cooling, it seems likely that the absolute values of the barriers for s/c and c/i in both directions are small. The absolute values of the barriers against k/i transitions in both directions are considered to be very high from the large ΔS^* , although the barrier against the transition from i to k is considered to be much higher than that against the reverse transition, resulting in the monotropy of the latter transition.

The behavior of ChP can be explained similarly to the case of ChS. The diagram of ChO is complex due to the existence of two crystalline phases, as analyzed previously by us,⁵⁾ but could be explained similarly in principle to the cases of ChS and ChP. The case of ChM is the simplest among our samples. Only the thermodynamically stable phases were found. However, taking into consideration the role of the kinetic barrier in each phase-transition we can expect under appropriate conditions that paths causing the appearance of various metastable phases or generally different paths from those of Chart 1 will appear. This may also be expected in the cases of ChP, ChS, and ChO.

Thermotropic Viscosity Change of Cholesteryl Esters with Continuous Heating and Cooling and their Accompanying Phase-Transitions

Previously,⁴⁾ we studied the rheological properties of ChM, ChP, and ChO at various temperatures and shear rates. We then assumed that these esters follow the same paths in the viscometric environment under mechanical shear as in the static environments of DSC and PM. However, this assumption would not hold if the deviation from the paths of Chart 1 occurred for the reason mentioned above with respect to the μ_{rel} vs. T diagrams. Therefore, by referring to the diagrams as well as the data of Table I, we examined the thermotropic phase behavior of these esters and ChS observed in this work under various thermal conditions. Rheological data from the previous work⁴⁾ were also considered.

The changes of viscosity, η , of ChM, ChP, ChS, and ChO with temperature on continuous heating and cooling are shown in Fig. 2(a), (b), (c), and (d), respectively, as plots of the logarithm of viscosity, $\ln \eta$, against inverse temperature, $1/T$. The transition temperatures determined by means of DSC are indicated by arrow-heads on the upper abscissas (abridged in the text as $T^*(\text{s/c})$ and so forth for the transitions from s to c, *etc.*). In addition, we supposed that no fluid change significantly affecting the internal structure and no phase-transition occur provided that the linear relation of $\ln \eta$ vs. $1/T$ holds according to Andrade's equation, Eq. 2, in the temperature region concerned:

$$\ln \eta = \ln B + U^*/RT \quad (2)$$

where B is a constant, R the gas constant and U^* the activation energy of flow. The above assumption might be weakened to allow a slight dependency of B upon T .

Cholesteryl Myristate—On Heating: At the point, X, in Fig. 2(a) or *ca.* 351 K, where we could start to read the value of η , ChM was in the state s or the like, because the

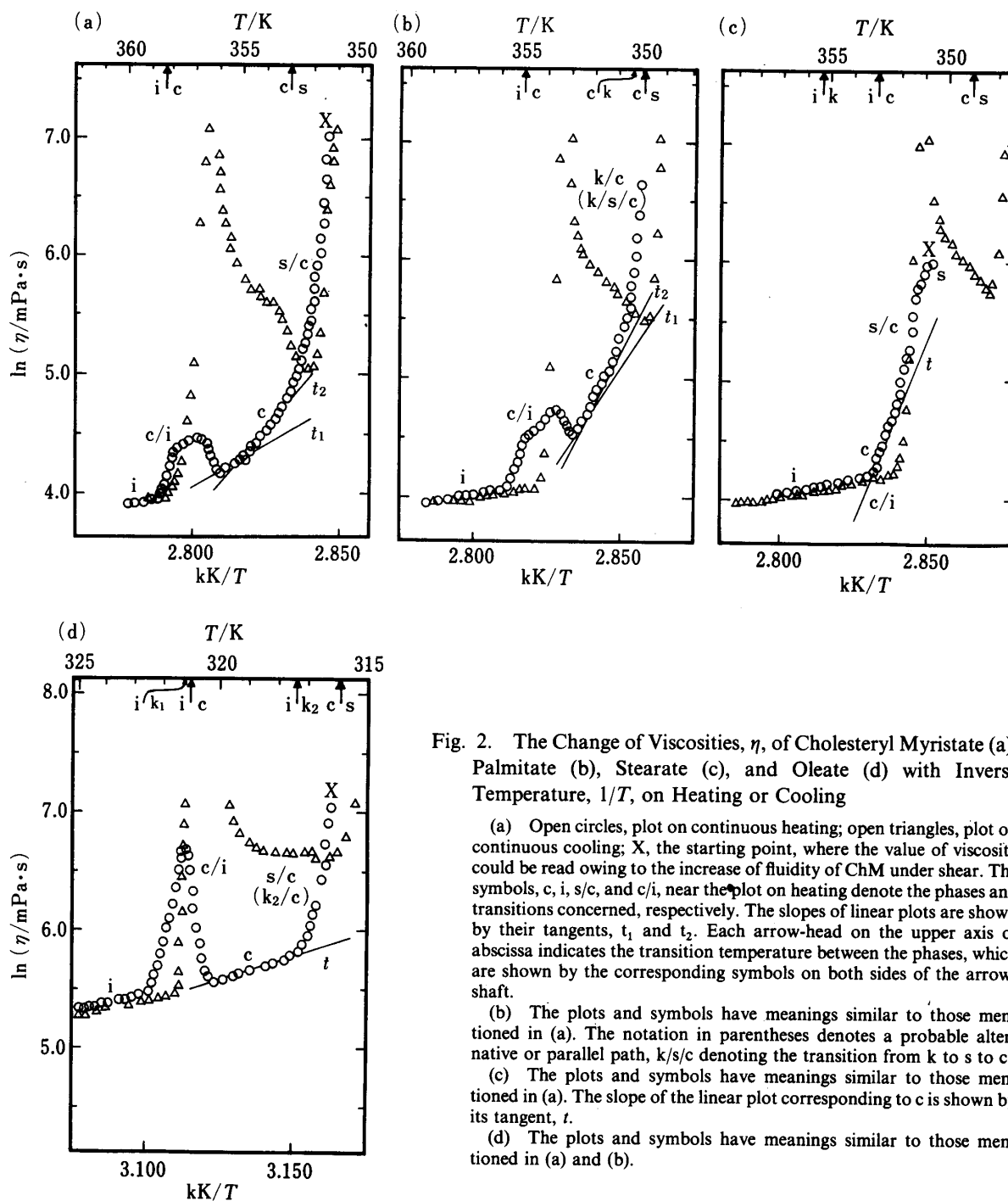


Fig. 2. The Change of Viscosities, η , of Cholesteryl Myristate (a), Palmitate (b), Stearate (c), and Oleate (d) with Inverse Temperature, $1/T$, on Heating or Cooling

(a) Open circles, plot on continuous heating; open triangles, plot on continuous cooling; X, the starting point, where the value of viscosity could be read owing to the increase of fluidity of ChM under shear. The symbols, c, i, s/c, and c/i, near the plot on heating denote the phases and transitions concerned, respectively. The slopes of linear plots are shown by their tangents, t_1 and t_2 . Each arrow-head on the upper axis of abscissa indicates the transition temperature between the phases, which are shown by the corresponding symbols on both sides of the arrow-shaft.

(b) The plots and symbols have meanings similar to those mentioned in (a). The notation in parentheses denotes a probable alternative or parallel path, k/s/c denoting the transition from k to s to c.

(c) The plots and symbols have meanings similar to those mentioned in (a). The slope of the linear plot corresponding to c is shown by its tangent, t .

(d) The plots and symbols have meanings similar to those mentioned in (a) and (b).

TABLE II. Activation Energy of Flow for Cholesteryl Esters, U^*

Ester	Myristate	Palmitate	Stearate	Oleate
$U^*/\text{kJ}\cdot\text{mol}^{-1}$				
i	33.5	37.8	43.5	50.7
c	265	409	527	67.2

temperature is sufficiently deep inside the appropriate region, limited by $T^*(k/s)$ and $T^*(s/c)$, and the viscosity was very high (one of the characteristics of s).²⁾ With increasing temperature, the viscosity plot showed a step decline at first, changed gradually to a gentle slope, formed a

hump and finally took a linear course. The last phase can be deduced to be *i* from the facts that its flow is Newtonian⁴⁾ and the temperature region in which it exists exceeds the value of $T^*(c/i)$. The value of U^* in this region is shown in Table II. The phase corresponding to the linear part just before the hump can be estimated to be *c* from its existence between $T^*(i/c)$ and $T^*(c/s)$ and its low viscosity, which is the distinctive feature of *c*,²⁾ in comparison with *s*. On detailed inspection, however, the curve was found to consist of two lines, whose tangents are shown in Fig. 2(a) as t_1 and t_2 , respectively. We assigned the linear portion with t_2 to *c* and considered the portion with t_1 to be influenced by the hump. Then, the value of U^* in *c* was obtained from t_2 and is shown in Table II. The non-Newtonian flow⁴⁾ of ChM in *c* is considered to be related to the higher U^* in *c*. Concerning the region for *s*, we supposed it would be observed in the upper-right part of Fig. 2(a) as a gentle slope connecting X with a bend in between, if viscosity measurement beyond X were possible. This supposition was based on the fact that at lower shear rates, where the higher viscosity could be measured by our viscometer, the above-mentioned gentle slopes were observed for ChM,⁴⁾ as well as on the expectation that the viscosity in *s* would also follow Eq. 2. The possibility of *k* in this region was excluded by the fact that the temperature of measurement was higher than $T^*(k/s)$.

From the above discussion, it is concluded that the steep decline with X included corresponds to the transition region between *s* and *c*, and the hump corresponds to the transition region between *c* and *i*. Generally, liquid crystal has a dual nature, continuum and swarm,^{2c} and its state as well as the property to be observed determine which is dominant. In the transition region of *s/c* under shear, ChM is considered to behave as a swarm, a gathering of sub-structures, each of which is *s* or *c*; with increase of the temperature, the ratio of sub-structures in *s* decreases. The mechanical agitation induced by the shearing force is supposed to favor the swarm structure of ChM and also to hasten the *s/c* transition a little below $T^*(s/c)$. Early arrival of the *s/c* transition might easily be caused by the chemical potential jump from *s* to *c*, since it is so small near $T^*(s/c)$, as seen in Fig. 1; the energy for this could be provided by the mechanical shearing force of the viscometer. Generally speaking, any mechanical force is considered to break down the structure of a material and bring it into the state with higher entropy in terms of thermodynamics. In the case of ChM, it transfers from the phase with smaller slope of μ_{rel} vs. T , *s*, to the phase with larger slope, *c*, as seen in Fig. 1(a). In the transition region from *c* to *i*, where the hump was observed, we can expect a certain discontinuity of the internal structure of ChM. However, taking into consideration the facts that the sub-structure size and shape depended upon the shear rate,⁴⁾ we shall postpone a discussion on the region of hump formation until the later kinetic treatment of viscosity measurements. For the time being, we may regard the hump only as reflecting a peculiar internal structure of ChM.

On Cooling: The formation of the peculiar structure at *i/c* (differing from *c/i* only in direction) as well as the phase *c* itself and the transition *c/s* were considered to be delayed by the kinetic barriers in the production of embryos to new phases or structures. As a result, the region for *c* was so narrowed that the existence of *c* was identified near $T^*(c/s)$ only as the minimum of the $\ln \eta$ vs. $1/T$ curve. The hump or peak on cooling at *i/c* became significantly high, reflecting the greater growth of the peculiar structure as compared with that on heating.

Cholesteryl Palmitate—On Heating: ChP was temporarily held at *ca.* 360 K in the viscometer, then cooled to *ca.* 323 K for the start of measurement on heating and its phase was considered to change from *i* to *c* to *s* and finally to *k* through the paths shown in Chart 1. Some ChP might remain in *s* at the start. On heating and under agitation from the shearing force of the viscometer, ChP would change from *k* to *c* with an increasing ratio of *c* and one kind of suspension or swarm consisting of *k* and *c* would result in the same way as with ChM in *s/c*. The delay of viscosity reading, which is shown by the rather low position of X in Fig. 2(b), suggests a scaffolding structure, which is constructed from finely dispersed and

interacting k particles as the scaffold and c phase as the interstitial medium. The phase s , which might remain at the start or appear through the k/s transition induced by the chemical potential jump, can be considered to participate in the above structure. The scaffolding structure is considered to be the same as proposed by Wo. Ostwald⁹⁾ to account for anomalous or structural viscosity. The steep decline of $\ln \eta$ vs. $1/T$ from X was considered to reflect the above-mentioned k/s transition, which might include k/s and succeeding s/c transitions. The other features of the $\ln \eta$ vs. $1/T$ plot of ChP may be interpreted similarly to the case of ChM. The values of U^* for c and i are shown in Table II. The former was calculated from the tangent with t_2 .

On Cooling: Similar processes to the case of ChM are considered to occur.

Cholesteryl Stearate—On Heating: At the start of the viscosity measurement on heating, the phase of ChS was considered to change to k in the same way as in the case of ChP. From X, where viscosity reading was possible, the $\ln \eta$ vs. $1/T$ plot followed a course similar to those of ChM and ChP, but without the appearance of a hump. Since the meeting of the second-last linear plot with the last occurred just at $T^*(c/i)$, these plots can be assigned to c and i , respectively. Therefore, the steeply declining plot, at least in the later stage, must represent the transition, whose final state is c . Since the starting phase of viscosity measurement was estimated to be k , the initial state of the above transition might be considered to be k . However, the bend preceding the steep decline suggests an intermediate phase between k and c . Thus, we supposed that the bend and the steep decline can be assigned to s and s/c , respectively. This implies that the mechanical agitation in the viscometer provided the energy for the chemical potential jump of ChS from k to s , that a scaffolding structure of k and s , with an increasing ratio of s , was formed in the region between the start of viscosity measurement and X, and that the ChS became completely s and started to flow to make the viscosity reading possible at X. There is the possibility that a certain amount of ChS remained in s at the start of viscometry on heating. The values of U^* for c and i obtained from the slopes in Fig. 2(c) are shown in Table II.

On Cooling: Processes similar to those in the cases of ChM and ChP are considered to occur for ChS on cooling. The hump for i/c reappeared.

Cholesteryl Oleate—On Heating: ChO was temporarily held at *ca.* 329 K in the viscometer, then cooled to *ca.* 312 K for the start of viscometry on heating; its phase was considered to change from i to c to s . Since we heated ChO for viscometry immediately after cooling finished, the presence of k_1 and k_2 is considered to have been avoided by virtue of their very slow or difficult formation near or above 312 K, as estimated from the DSC and PM observation.⁵⁾ Therefore, the plot of ChO in Fig. 2(d) can be discussed similarly to the case of ChM. However, the appearance of the steep decline above $T^*(s/c)$ suggests the possibility that the formation of k_2 from s was induced by the viscometric agitation and k_2/c transition occurred before the normal k_2/i , producing the steep decline near $T^*(k_2/c)$, which is estimated to exist between $T^*(s/c)$ and $T^*(k_2/i)$ in Fig. 1(d). Also, in comparison with ChM, ChO has a sharper hump and an almost perfectly linear plot for c with a unique tangent, t . The values of U^* for c and i are shown in Table II. The path through k_2/c is indicated in parentheses in Fig. 2(d), as a probable one.

On Cooling: Similar processes to the cases of ChM, ChP, and ChS are considered to occur.

Intrinsic and Steady-State Viscosities of Cholesteryl Myristate and Oleate at Various Temperatures from the Measurements of Isothermal Viscosity Relaxation

From the difference of results between the preceding experiments on heating and on cooling, it can be concluded that the thermal history affects the viscometric behavior of cholesteryl esters. Also, the internal structures of esters were considered to be liable to break

down during viscometry. We therefore attempted to estimate the viscosity which each ester has independently of its thermal history and in its equilibrium or steady-state before and sufficiently after viscometric agitation; these will be referred to as intrinsic viscosity, η_i , and steady-state viscosity, η_s , respectively.

In the first series of experiments, as follows, we examined the effect of thermal history on the viscometric behavior of ChM, which has the simplest transition paths among our esters, as can be seen in Chart 1. Three kinds of thermal histories or pretreatments before the viscosity measurements were chosen. The measurements themselves were carried out under isothermal conditions at a constant shear-rate of 10 s^{-1} .

Method I—After heating ChM to the state i, we cooled it down at *ca.* 0.6 K min^{-1} to any prescribed temperature, T , and immediately started the viscosity measurement.

Method II—After heating ChM to the state i, we cooled it down at *ca.* 0.6 K min^{-1} to 323.15 K , heated it again without delay at *ca.* 0.5 K min^{-1} to T and immediately started the measurement.

Method III—The same method as II, except that 1 h of ageing was added at 323.15 K before reheating.

The viscosity change at 355 K of ChM, which was pretreated by method I or II, is shown in Fig. 3, as a plot of $\ln \eta$ vs. time, t . The result by method III was almost the same as that by method II. All other results showed qualitatively similar time-courses to the results shown in Fig. 3, irrespective of the kind of pretreatment and the variation of T . Since the value of η at

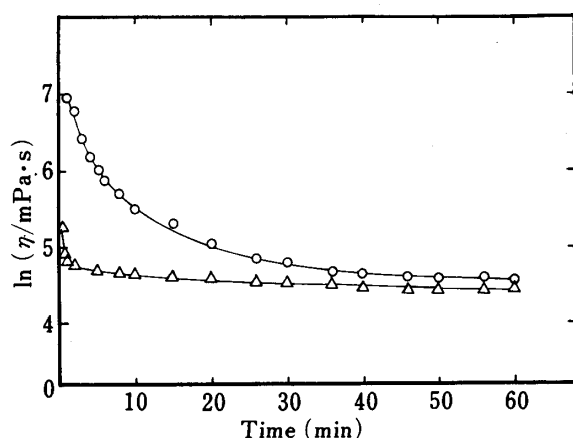


Fig. 3. Isothermal Viscosity Time-Courses of Cholesteryl Myristate at 355 K

Logarithmic viscosity after the start of viscometry is denoted by open circles or triangles, which correspond to method I or II as a thermal pretreatment, respectively.

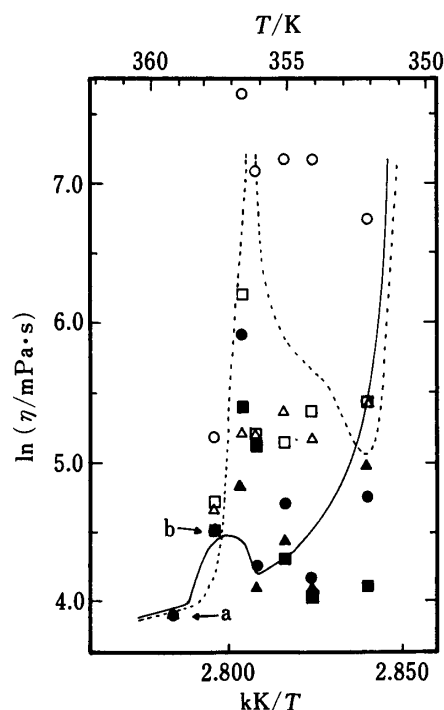


Fig. 4. Intrinsic and Steady-State Viscosities of Cholesteryl Myristate at Various Temperatures without Isothermal Ageing

Logarithms of intrinsic viscosity, η_i , and steady-state viscosity, η_s , are plotted against $1/T$. Open symbols, η_i ; filled symbols, η_s . Thermal pretreatment: circles, method I; triangles, method II; squares, method III. Superimposed plot is indicated by an arrow with a or b: arrow with a, all kinds of symbols; arrow with b, all filled symbols. Solid and dotted curves denote the viscosity changes on continuous heating and cooling, respectively, as shown in Fig. 2(a).

the start, *i.e.* $t=0$, is not affected yet by the agitation owing to viscometry, it can be regarded as η_i . The value of η after a sufficient lapse of time or 1 h in the plots of Fig. 3 can be regarded as η_s . The values of η_i and η_s , thus obtained, at various T are plotted in Fig. 4 in the same form as in fig. 2(a). As each value of η_i was usually difficult to determine due to the rapid decrease of η near the start of viscometry, it was estimated by the extrapolation of the η vs. t relation to $t=0$.

Generally, the time course of η for ChM obeyed approximately the following equation, which is a modification that of Tiu and Boger¹⁰⁾:

$$\frac{d\eta}{dt} = k(\eta - \eta_s)^n \quad (3)$$

where $d\eta/dt$ is the rate of viscosity change with t , and k and n denote empirical constants. The relaxation of η during viscometry was considered to be caused by breaking the internal structures of ChM in various phases. As can be seen in Fig. 4, the value of η in i did not change, suggesting the absence of such an internal structure. In other phases, the difference between η_i and η_s was remarkable, especially in c. There, the effect of viscometric agitation on the internal structure of ChM seems to be significant. However, from a comparison of the results after different pretreatments, the effect of thermal history was also considered to be important, especially on the values of η_i . The value of η_i was higher in method I than in methods II and III, suggesting that ChM pretreated according to method I retained the internal structure which was formed at higher temperatures than the measured temperature, T , while those with methods II and III retained the internal structure formed at lower temperatures than T . In order to reduced or simplify the effect of thermal history, we modified methods I, II, and III by adding 1 h of ageing at T before the start of viscometry or agitation. Using the modified methods, *i.e.* methods I', II', and III', respectively, we measured the viscosity time-courses; the results are shown in Fig. 5 with the values of η_i and η_s . In comparison with the values of Fig. 4, the effect of thermal history on the values of η_s diminished significantly, but the difference in η_i still remained, although it was considerably reduced. Taking into consideration the still-remaining effect of thermal history, we preferred the results in Fig. 5 to those in Fig. 4, because the former showed more regular tendencies than the latter. It should be noted here that the viscosity plots at lower shear rates, which were reported previously,⁴⁾ showed curves intermediate in form and position between those obtained with methods I' and II' or III'. Generally speaking, from the higher values η_i than η_s , the internal structures of ChM in c as well as in the hump region are considered to be easily destroyed by viscometric agitation. The internal structure relating to the hump seems to exist in the absence of viscometric agitation and to break down with it, tending to rule out the turbulence theory proposed by Lawrence,⁷⁾ contrary to the discussion of Wo. Ostwald.⁹⁾ From the results of viscometry under continuous heating and cooling as well as under isothermal conditions, the hump seems to become larger with the transition from i to c than with that from c to i, suggesting significantly different internal structure from the structure of ChM in c and also suggesting that the structure is continuous or homogeneous in molecular terms. The highly viscous property might be attributed to a network-type structure, which is constructed out of molecules or small molecular aggregations interacting with each other in the same manner as in water or glycerol.

Results similar to those with ChM were obtained for ChO, as shown in Fig. 6. The similarity of U^* among η_i , η_s , and η on continuous heating suggests a common nature of fluidity, irrespective of the different structures depending on thermal and shearing history. We supposed tentatively that the identical value of U^* reflects the same structure of ChO in c in terms of molecular interaction and that the structure in c is continuous or homogeneous without shear, although the structure is different from that in i. The decrease of absolute

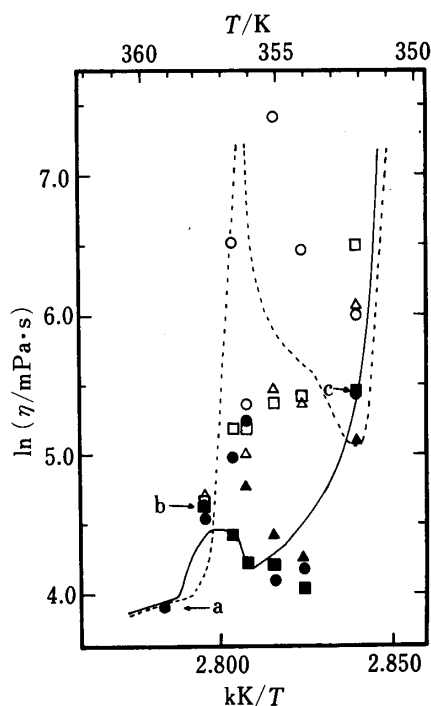


Fig. 5. Intrinsic and Steady-State Viscosities of Cholesteryl Myristate at Various Temperatures with One Hour of Isothermal Ageing

The plots and symbols have meanings similar to those mentioned in Fig. 4, except for the following. Circles, triangles, and squares denote methods I', II', and III', respectively, as thermal pretreatments. Arrow with a, all kinds of symbols; arrow with b, filled triangles and squares; arrow with c, filled circles and squares.

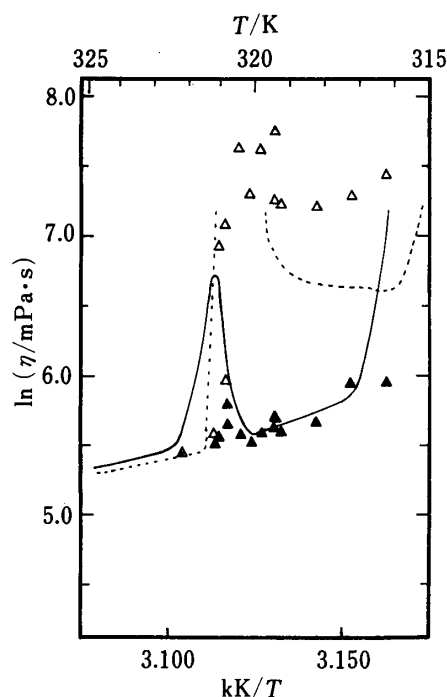


Fig. 6. Intrinsic and Steady-State Viscosities of Cholesteryl Oleate at Various Temperatures with One Hour of Isothermal Ageing

Method I' was adopted as a thermal pretreatment. Open symbols, η_i ; filled symbols, η_s . Solid and dotted curves correspond to the viscosities on continuous heating and cooling, respectively, as shown in Fig. 2(d).

viscosity under shear suggests that the continuous structure in c breaks down from its combined state to a gathering of independently moving substructures, *i.e.* a swarm. Similar circumstances would be expected for the other esters.

Further Discussion on the Hump Studied by Viscometry and NMR

From the inspection of Fig. 2 and Table II, we found a qualitative inverse correlation between the ease of hump formation and the value of U^\ddagger . While molecules in i can move in all directions in space with low energy barriers, molecules in c can move in one direction with a lower energy barrier than in the other two directions.²⁾ In other words, at the transition between c and i, molecules melt or freeze with respect to the motions in the above-mentioned directions. We supposed that the hump reflects a transition structure which is formed when molecules pass over the barriers and that molecules in c moving in one direction in spite of its higher energy barrier, U^\ddagger , might more easily clear the transition barrier at c/i.

As the discussion of viscometry was in terms of molecular motion, we measured the ¹³C-NMR spectroscopic behavior of ChO, which can be more easily examined owing to its fluidity at lower temperature as compared with other esters. However, our results have only confirmed the pioneering work of other authors.¹¹⁾ From the measurements of chemical shift, spin-lattice relaxation time, and line-width, we could not find any significant discontinuity in the transition region between c and i, although the behavior of ChO in c changes gradually from that in i as the temperature falls below $T^*(i/c)$. Therefore, we concluded that no special structure exists for the hump region as far as short-range molecular interactions are concerned. For further discussion on this problem, more precise measurements of NMR

changes with respect to temperature as well as frequency seem to be necessary. Acoustical studies might also be required.

References and Notes

- 1) For liquid-crystalline systems, we use the terminology proposed by Kelker and Hatz.^{2a)}
- 2) a) H. Kelker and R. Hatz, "Handbook of Liquid Crystals," Verlag Chemie, Weinheim, 1980, Chapt. 1; b) *Idem, ibid.*, 1980, Chapt. 12; c) *Idem, ibid.*, 1980, Chapt. 3.
- 3) a) I. Miyata and H. Kishimoto, *Yakugaku Zasshi*, **98**, 689 (1978); b) *Idem, ibid.*, **98**, 1629 (1978); c) *Idem, Chem. Pharm. Bull.*, **27**, 1412 (1979).
- 4) I. Miyata and H. Kishimoto, *Chem. Pharm. Bull.*, **28**, 619 (1980).
- 5) H. Kishimoto, T. Iwasaki, and M. Yonese, *Chem. Pharm. Bull.*, **33**, 1782 (1985).
- 6) K. Sakamoto, R. S. Porter, and J. F. Johnson, "Liquid Crystals II," ed. by G. H. Brown, Gordon & Breach Sci., Publ., London, 1969, pp. 237—249.
- 7) A. S. C. Lawrence, *Trans. Farad. Soc.*, **29**, 1080 (1933).
- 8) B. Tamamushi and M. Matsumoto, "Liquid Crystals and Ordered Fluids," Vol. 2, ed. by J. F. Johnson and R. S. Porter, Plenum Press, New York, 1974, pp. 711—721.
- 9) Wo. Ostwald, *Trans. Farad. Soc.*, **29**, 1002 (1933).
- 10) C. Tiu and D. V. Boger, *J. Texture Studies*, **5**, 329 (1974).
- 11) a) R. M. C. Mathews and C. G. Wade, *J. Magn. Reson.*, **19**, 166 (1975); b) J. A. Hamilton, N. Oppenheimer, and E. H. Cordes, *J. Biol. Chem.*, **252**, 8071 (1977); c) G. S. Ginsburg, D. M. Small, and J. A. Hamilton, *Biochem.*, **21**, 6867 (1982).